JOM 23029

Sterically overcrowded or charge perturbed molecules

XXIII *. Hexakis(trimethylsilyl)disilane: structure and photoelectron spectrum of a sterically overcrowded molecule **

Hans Bock, Jochen Meuret and Klaus Ruppert

Chemistry Department, University of Frankfurt, Niederurseler Hang, W-6000 Frankfurt / Main 50 (Germany)

(Received March 16, 1992)

Abstract

Hexakis(trimethylsilyl)disilane [$(H_3C)_3Si]_3Si–Si[Si(CH_3)_3]_3$ crystallizes in the rhombohedral space group $R\bar{3}c$ with six molecules of D_3 symmetry per unit cell. The steric overcrowding by the 18 peripheral methyl groups shows up especially in the elongation of the central SiSi bond to 240 pm, in the differing dihedral angles ω(SiSi–SiSi) of 43° and 77° and in the rather short non-bonded C $\cdots$ C distances of only 352 pm, which reveals an inter-penetration of the methyl groups within their van der Waals radii of about 200 pm. The ^1H nuclear magnetic resonance (NMR) spectrum in DCCl$_3$ at 190 K, however, does not exhibit any signal splitting of the 42 equivalent methyl hydrogens and so the rotational barriers must be below 20 kJ mol^{-1}. The photoelectron spectrum shows in its low-energy region between 7.2 eV and 9.3 eV a resolved α_{SiSi} ionization pattern, which can be satisfactorily reproduced by a LCBO–MO model parametrized in terms of the different SiSi/SiSi bond interactions, and the higher ionization energies are assigned on the basis of a radical cation state comparison with [$(H_3C)Si]_3SiCl$, $(H_3C)_3SiCl$ and $(H_3C)_3CCl$. Although the first vertical ionization energy is only 7.70 eV, which is the lowest observed so far for a disilane derivative, and in accord with the cyclovoltammetrically determined irreversible first oxidation potential, no persistent radical cation of hexakis(trimethylsilyl)disilane can be generated in solution.

1. Introduction

As long as 25 years ago numerous compounds containing the space-filling tris(trimethylsilyl)silyl group were synthesized by Gilman and coworkers [3]. The title compound is accessible either by Mg coupling of the chloride (Me$_3$Si)$_3$SiCl [3d] or, advantageously (*cf.* experimental section), by lithiation of the pentasilane followed by reaction with 1,2-dibromoethane [3e]:

$$Si[Si(CH_3)_3]_4 \qquad Cl-Si[Si(CH_3)_3]_3$$

(1)
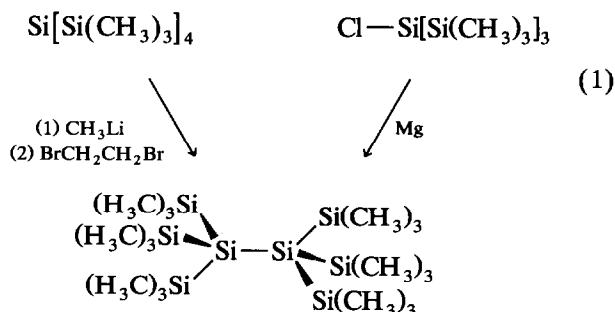
Subsequently, a great variety of other molecules with bulky [$(H_3C)_3Si]_3Si$ substituents have been prepared and investigated. Thus tris(trimethylsilyl)acylsilanes $(R_3Si)_3Si-C(=O)-R'$ were found to rearrange photochemically to the corresponding silaethylenes $(R_3Si)_2Si=Cr'OSiR_3$, which can be isolated if R' is a sterically shielding alkyl group such as adamantyl [4]. Its crystal structure reveals an elongated Si=C double bond of length 176 pm as well as a twisting of the two molecular halves by 15°, presumably due to steric strain exerted by the bulky ligands [4]. Other representative examples selected from the extensive literature covering tris(trimethylsilyl)silyl compounds, further illustrate the shielding effect of $(R_3Si)_3Si$ substituents to stabi-

---

Correspondence to: Professor H. Bock.

* For Part XXII see ref. 1; see also ref. 2.
** Dedicated to Professor R. West on the occasion of his 64th birthday; see also Ref. 32.

lize otherwise reactive intermediates. More recently, for instance, both the thermally stable linear imino-borane $(R_3Si)_3Si-B\equiv N-CR_3$ with its rather short $B\equiv N$ bond of 122 pm [5], and the first formylsilane $(R_3Si)_3Si-C(=O)-H$ [6], which can be kept unchanged for some weeks under nitrogen, have been isolated. Furthermore, the now commercially available $(R_3Si)_3$-SiH is used in organic synthesis as a reducing reagent [7].

In contrast, aspects of both the electronic and steric perturbations of parent systems by $[(H_3C)_3Si]_3Si$ sub-stituents and their interplay, as well as the molecular dynamic aspects involved still remain to be investigated. However, the first electron diffraction study of such an overcrowded molecule [8], that of the moth-ball-shaped $Si[Si(CH_3)_3]_4$, which has a melting point of 534 K, revealed the following structural parameters: $d_{SiSi} = 236$ pm, $d_{SiC} = 189$ pm, $d_{CH} = 112$ pm, angle SiSiSi $= 111°$, angle SiSiC $= 108°$, angle SiCH $= 109°$ as well as the non-neighbour distances $d_{Si \cdots Si} = 386$ pm, $d_{C \cdots H} = 305$ pm, $d_{H \cdots H} \approx 260$ pm [8]. Its overall symmetry is reduced to T due to a torsional twist of the $Si(CH_3)_3$ groups by $11°$, and their internal rotation, although restricted by steric interlocking, is still possible.

Interpretation of the single crystal structures determined for numerous organometallic tris(trimethylsilyl)-silyl compounds [9-15], however, is less clear-cut. Comparison of the structures of the closely related manganese and rhenium pentacarbonyls, $[(H_3C)_3Si]_3Si$-$Me(CO)_5$ and $(H_3C)_3SiMe(CO)_5$, reveals that the bulkier ligand stretches the Si-Me bonds, which differ in length by 11 pm (Ref. 9: Si-Mn 256 pm and Si-Re 267 pm), each by the same amount of 7 pm. This observation suggests that there is a dominant electronic substituent effect, because the replacement of R_3Si by $(R_3Si)_3Si$ widens the angles SiReC to the adjacent carbonyl groups only slightly from $85°$ to $88°$, and the angles MnSiSi and ReSiSi are both $113°$. Further comparison with $Zn(Si[Si(CH_3)_3]_3)_2$ [10], which has linear Si-Zn-Si bonds of 234 pm length and Zn-SiSi angles of only $107°$, shows that the $Si(CH_3)_3$ groups are bent towards, rather than away from, the metal center. An attempt to use the angles XSiSi as a general indicator of steric repulsions [11] between the bulky groups in usually skew conformation, however, fails: in the sterically overcrowded zirconium derivative $[(H_3$-$C)_3Si]_3SiZr[OC(CH_3)_3]_3$ they are approximately tetra-hedral (Ref. 12a: $110°$ and $111°$) as they are also in the gold(I) compound $[(H_3C)_3Si]_3Si-AuP(C_6H_5)_2CH_3$ (Ref. 12b: $111°$). They differ considerably, however, in $[(H_3C)_3Si]_3Si(R_2N)_2Mo\equiv Mo(NR_2)_2Si[Si(CH_3)_3]_3$ (Ref. 13a: $105°$ and $115°$) and in $[(H_3C)_3Si]_3Si-Sn(Cl)_2$-$Si[Si(CH_3)_3]_3$ (Ref. 13b: $105°$ and $110°$), which also has

a rather large angle SiSnSi of $143°$. Sometimes, they can be unexpectedly small, as in the iminoborane $[(H_3C)_3Si]_3SiB\equiv N-C(CH_3)_3$ ([5]: $102°$). In compounds with a distance of more than 400 pm between the two $[(H_3C)_3Si]_3Si$ half-shells [1,14], such as the novel 1,4-disubstituted benzene derivative, $[(H_3C)_3Si]_3SiC_6H_4Si$-$[Si(CH_3)_3]_3$, there is no steric overcrowding between the two halves of the molecule.

Noteworthy in this context is the very large increase in steric congestion brought about by introduction of tris(trimethylsilyl)silyl groups in place of tris(t-butyl)silyl groups. Owing to the considerably shorter SiC bonds, for instance, the SiSi bond in $[(H_3C)_3C]_3SiSi[C(CH_3)_3]_3$ is stretched by 35 pm to 270 pm [15a], or in the respective disiloxane, $[(H_3C)_3C]SiOSi[C(CH_3)_3]_3$, the angle SiOSi is opened relative to that in the hexam-ethyl derivative by $32°$ resulting in a linear Si-O-Si skeleton [15b]. Smaller, but still recognizable effects of steric overcrowding are found in compounds with "reverse" silylalkyl substituents $[(H_3C)_3Si]_3C$ such as hex-akis(trimethylsilyl)-2-butyne, $[(H_3C)_3Si]_3C-C\equiv C-C[Si(CH_3)_3]_3$, in which the two molecular halves are about 400 pm apart [16].

In order to contribute to the discussion of the electronic as well as the steric effects of the $[(H_3C)_3Si]_3Si$ group, molecules of higher symmetry are obviously of advantage. Therefore, we have chosen hexakis(trimeth-ylsilyl)disilane $[(H_3C)_3Si]_3SiSi[Si(CH_3)_3]_3$ and report here on its crystal structure and its photoelectron spectrum [2]. *

2. Experimental section

2.1. Hexakis(trimethylsilyl)disilane [3e]

To a solution of 6.15 g (19.2 mmol) of tetrakis(tri-methylsilyl)silane in 45 ml of anhydrous THF at 273 K and under Ar in a baked-out three-necked flask were added 24 ml of a 0.8 molar $LiCH_3$ in ether (19.2 mmol). After stirring for 1 d at 300 K, the then yellow-brown solution was cooled to 200 K and 0.83 ml of 1,2-dibromoethane (1.8 g, 9.6 mmol) were added drop-wise. During 4 h stirring at the same temperature ethylene was evolved and the mixture became cloudy. Treatment with 50 ml of H_2O at 273 K, was followed by extraction with diethyl ether. The extract was dried and evaporated, and the residue recrystallized from acetone to give 2.8 g (58%) white, air-stable crystals,

* Since the submission of this paper we have learned that the structure of hexakis(trimethylsilyl)disilane has also been determined both by S.P. Mallela, I. Bernal and R.A. Geanangel, Inorg. Chem., 31 (1992) 1626 as well as by F.R. Fronczek and P.D. Lickiss, Acta Crystallogr. C, in press. For our preliminary communication see ref. 18.

TABLE 1. Atomic coordinates and equivalent isotropic displacement factors [a]

	x	y	z	U_{eq}
Si(1)	0	0	1975(1)	43(1)
Si(6)	−1540(1)	−574(1)	1559(1)	72(1)
C(61)	−2512(5)	−1691(6)	1914(4)	111(5)
C(62)	−1546(8)	−898(9)	760(4)	161(9)
C(63)	−1915(7)	361(7)	1593(5)	137(7)

[a] The molecule is highly symmetric; for better understanding the atoms are numbered clockwise without labelling of symmetry-equivalent atoms. There is a crystallographic three-fold rotation axis along the Si(1)–Si(2) bond relating Si(7) and Si(8) to Si(6). There are also crystallographic two-fold rotation axes perpendicular to and bisecting the Si(1)–Si(2) bond which relate the two ends of the molecule to each other. Thus the bond Si(1)–Si(2) would conventionally be written as Si(1)–Si(1′) where ′ is the symmetry element $y, x, \frac{1}{2} - z$.

m.p. = 645 K. ^{1}H NMR (CDCl$_3$, TMS): 0.30 ppm (s, 54H); MS: $m/e^- = 495$ (M$^+$), 480 (M$^+$− CH$_3$), 422 (M$^+$− Si(CH$_3$)$_3$).

2.2. Tris(trimethylsilyl)chlorosilane [3d]

A mixture of 2.45 g (9.85 mmol) of tris(trimethylsilyl)silane and 9.5 ml (15.2 g = 98.5 mmol) of anhydrous CCl$_4$ was refluxed under Ar for 2 h. After *slow* removal of the solvent, partly at 10^{-2} mbar, the colourless residue obtained was twice sublimed at 10^{-2} mbar to give the waxy [(H$_3$C)$_3$Si]$_3$SiCl in 95% yield (2.65 g; m.p. = 324 K). It was kept under dry Ar to avoid hydrolysis. ^{1}H NMR (CDCl$_3$, TMS): 0.24 ppm (s, 27H). MS: $m/e = 283$ (M$^+$), 268 (M$^+$− CH$_3$), 210 (M$^+$− Si(CH$_3$)$_3$).

2.3. Crystal structure analysis

C$_{18}$H$_{54}$Si$_8$ (MW: 495.31); rhombohedral space group $R\bar{3}c$ (No. 167), $Z = 6$, (300 K): $a = b = 1614.5$ (8), $c = 2285.9$ (13) pm; $\alpha = \beta = 90°$, $\gamma = 120°$; $V = 5153.2 \times 10^6$ pm^3 (300 K), $\rho_{calc.} = 0.955$ g cm^{-3}, μ(Mo Kα) = 3.1 cm^{-1}, Siemens AED-2 diffractometer, $3° < 2\Theta < 48°$, 3621 reflections of which 598 are independent with $I > 2\sigma(I)$. Direct methods (SHELXTL-PLUS), C and Si positions anisotropically refined (Table 1), H positions not detected; $R = 0.065$, $R_w = 0.067$; $w = 1/\sigma^2(F) + 0.0003F^2$, $N = 598$, $NP = 41$, $+0.34/ -0.21$ e Å^{-3}. The central SiSi bond is located on a threefold axis. Deviations in structural parameters (Fig. 1): ±0.9 pm and $\pm0.5°$. Further details of the crystal structure determination are available on request from the Fachinformationszentrum Karlsruhe, Gesellschaft für wissenschaftlich-technische Information mbH, W-7514 Eggenstein–Leopoldshafen 2 (Germany), on quoting the depository number CSD-56427 the names of the authors and the literature citation.

2.4. Instrumentation

2.4.1. ^{1}H NMR

Spectra were recorded with a 250 MHz Bruker AM 250 spectrometer at 300 and 190 K.

2.4.2. Photoelectron spectra

Recorded with the high-performance spectrometer Leybold Heraeus UPG 200, with that of hexakis(trimethylsilyl)disilane at a heated inlet temperature of 350 K. Data were handled on line via an Atary Mega ST2 connected to a VAX 11/750. For calibration, both
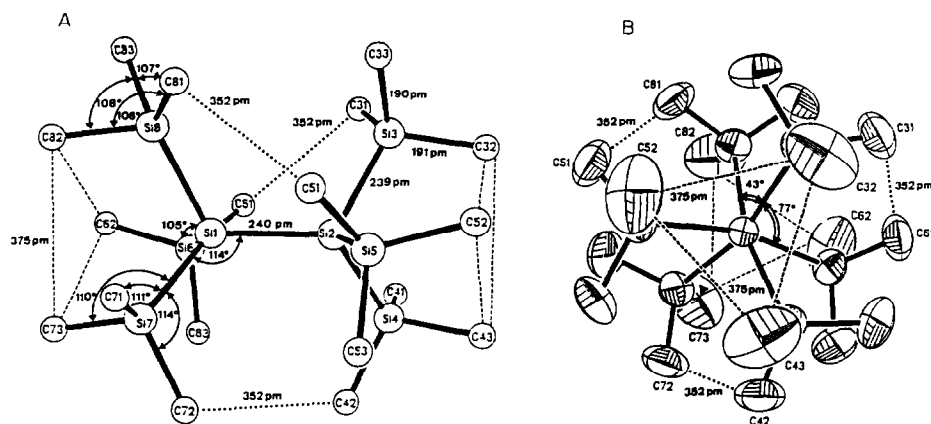

Fig. 1. Molecular structure of hexakis(trimethylsilyl)disilane. (A) The SiC skeleton viewed perpendicular to the plane containing the central SiSi bond and one of the C_2 axes with the numbering of Si and C centers as well as essential bond lengths and angles (Table 2). (B) View in the direction of the C_3 axis through the central bond with thermal ellipsoids (50%) and the dihedral angles (𝛿). In addition, the shortest distances (· · · · · ·, 352 pm and — — —, 375 pm) between nonbonded carbon centers are pointed out (cf. text).

TABLE 2. Selected structural parameters for hexakis(trimethylsilyl)
disilane D_3 including distances between nonbonded C centers (for
numbering, see Fig. 1A and Table 1, footnote)

Selected bond lengths (pm)			
Si(1)–Si(2)	240.5(5)	Si(6)–C(63)	188.7(14)
Si(2)–Si(3)	237.2(2)		
Si(6)–C(61)	190.1(10)	Si(6)–C(62)	188.1(8)

Selected bond angles (°)			
Si(1)–Si(2)–Si(3)	113.6(1)	Si(3)–Si(2)–Si(4)	105.0(1)
Si(2)–Si(3)–C(32)	110.7(4)	Si(2)–Si(3)–C(31)	114.2(3)
Si(2)–Si(3)–C(33)	111.3(3)		

the $\bar{X}(^2P_{3/2})$ ionizations of Xe at 12.13 eV and of Ar at
15.76 eV have been used.

2.4.3. Cyclic voltammetry

Performed by use of a combination of M 173, M 276
and the function generator M 175 supplied by EG & G
Princeton Applied Research; reference electrode
Ag/AgCl, counter electrode Pt, working electrode
glassy carbon (GCE). All solvents and the conducting
salt $Bu_4N^+ClO_4^-$ TBAP were carefully purified under
Ar and measurement were also under Ar.

2.4.4. (AM 1) Calculations [17]

Started from the structural parameters determined
and were carried out with the MOPAC program package,
kindly provided by Professor M.J.S. Dewar, Austin,
Texas, with optimized silicon parameters [17b] on an
IBM RISC 6000/320 H computer.

3. Single crystal molecular structure

The single crystal study at room temperature re-
vealed a rhombohedral unit cell of space group $R\bar{3}c$
containing six molecules. The shortest distances C · · · C
between carbon centers of different molecules are 389
pm; below the sum of the interference radii of two
methyl groups (ref. 18: 400 pm), which thus must be
partly interlocked and indicate some Van der Waals
bonding C–H · · · H–C between their hydrocarbon
spheres.

The title compound, $[(H_3C)_3Si]_3SiSi[Si(CH_3)_3]_3$, has
an SiC skeleton which as shown by the differing dihe-
dral angles of 43 and 77° (Fig. 1B and Table 2) exhibits
D_3 symmetry. As expected (cf. Introduction), its 18
peripheral methyl groups do cause distortions due to
steric overcrowding. Despite the cogwheel-like gearing
of both molecular halves, three pairs of methyl group C
centers (Fig. 1A: C31/61, C42/72 and C51/81) display
nonbonded distances of only 352 pm. In view of the
usual interference radius for freely rotating H_3C sub-
stituents of 200 pm [18], even if their C–H bonds are
interdented, there must be some steric compression
and presumably also peripheral H · · · H van der Waals
bonding. There are, in addition, six C · · · C distances
of 375 pm (Fig. 1B) that are also shorter than 400 pm.
The resulting spatial overcrowding stretches both the
central and the adjacent σ_{SiSi} bonds to 240 and 239 pm
length (Fig. 1A and Table 2), which are, except for the
hexakis (t-butyl) derivative [15], longer than those found
for most of the other structurally characterized disilane
derivatives [19–23]. See Table 3, which gives structural
data for some disilane derivatives X_3SiSiX_3 deter-
mined by X-ray diffraction [15] or by electron diffrac-
tion in the gas phase [19–23] (dihedral angles in brack-
ets: determined for best curve fit starting from as-
sumed D_{3d} symmetry). In addition, interference radii
$r^{Int.}(X)$ of substituents X [18] are given as well as
estimates of rotational barriers $\Delta H_{Rot}^{\ddagger}$ around the cen-
tral SiSi bonds [20].

Disilane and its simple derivatives (Table 3: X = F,
Cl, CH_3) show Si–Si bond lengths between 232 and
234 pm, normal tetrahedral angles around the Si cen-
ters and probably [20,23] staggered conformations of
D_{3d} symmetry. The rotational barriers are rather low;
they increase considerably on shortening of the central
bond, as demonstrated by the sequence from Cl_3Si–
$SiCl_3$ (Table 3: $\Delta H_{Rot} \approx 4$ kJ mol^{-1}) via Cl_3Si–CCl_3
(ref. 24: 18 kJ mol^{-1}) to Cl_3C–CCl_3 (ref. 24: 45 kJ
mol^{-1}). For the title compound, the ^1H NMR spec-
trum at 190 K showed no splitting of the sharp singulet
signal flanked by ^{29}Si as well as ^{13}C satellites (cf.
experimental section) and so the rotational barrier

TABLE 3. Structural data for some disilane derivatives

X_3Si–SiX_3		X				
		H [19]	F [20,21]	Cl [22]	CH_3 [23]	$C(CH_3)_3$ [15]
d_{SiSi}	(pm)	233.1	231.7	232.4	234.0	269.9
γ(SiSiX)	(°)	110.3	108.6	109.7	108.4	112.0
ω(XSi–SiX)	(°)	(60)	(60)	(60)	($\approx$ 60)	45/75
$r_{Int.}$(X)[18]	(pm)	120	135	180	200	350
$\Delta H_{Rot}^{\ddagger}$[20]	(kJ mol^{-1})	< 2	$\approx$ 2	$\approx$ 4		

around the central Si–Si bond must also be < 20 kJ mol^{-1}.

All molecules studied so far that exhibit rather long Si–Si bonds due to steric strain such as hexakis(t-butyl)disilane [15] (Table 3: 270 pm), hexakis (t-butyl)-cyclotrisilane (ref. 25: 251 pm), and hexakis (t-butyl)-1,3-diiodotrisilane (ref. 26: 258 pm and 264 pm), show additional structural distortions. Some anomalies are also found for hexakis(trimethylsilyl)disilane (Fig. 1A and Table 2): for example, the angle Si2 Si1 Si7 = 114° is larger and the adjacent angle Si6 Si1 Si8 = 105° smaller than tetrahedral. On the other hand, the average Si–C bond lengths of 190 pm are comparable with those in Si(CH$_3$)$_4$, 188 pm [23], and Si[Si(CH$_3$)$_3$]$_4$, 189 pm [8].

Important criterions for steric overcrowding in all disilane derivatives with a C_3 substituent axis are obviously the differing dihedral angles and their deviation from the 60° value that characterizes the perfectly staggered conformation of D_{3d} skeletal symmetry. In some of the gas-phase electron diffraction studies of disilane derivatives (Table 3, X = F [20,21] or CH$_3$ [23]) the information may be less clear-cut because D_{3d} "staggering" was assumed as the starting point for the curve-fitting. However, the crystal structures of the isovalence electronic hexakis(trimethylsilyl)- and hex-akis(t-butyl)-substituted organodisilanes reveal considerably differing dihedral angles of comparable magnitude, ω(SiSi–SiSi) = 43° and 77° (Fig. 1B and Table 2) as well as ω(CSi–SiC) = 45° and 75° [15] (Table 3). This observation can be rationalized in terms of energetically favorable cogwheel-like gearing of the methyl groups, which is indicated in Fig. 1B by dotted and hatched lines connecting non-bonded carbon centers in different (H$_3$C)$_3$Si substituents (Fig. 1B): They represent three "inner" distances of only 352 pm, and six somewhat longer "outer" ones of 375 pm, which are both well within the 400 pm range given by the sum of the interference radii for two methyl groups [18]. It should be emphasized that the replacement of six longer Si–Si by the six shorter Si–C bonds in the t-butyl derivative leads to considerably increased steric overcrowding, which results in the extreme value of 270 pm for the central Si–Si bond and in considerable stretching of the Si–C bonds, each of 199 pm length [15].

In conclusion, reduced Pauling bond orders, lg(PBO) = [d(1) − d(x)]/60 [27], for sterically elongated SiSi bonds [25,26] are indicated: thus for the longest Si–Si bond observed so far, that of 270 pm length in hexakis(t-butyl)disilane, a value of only 0.26 is indicated [15]. For the less sterically compressed trimethylsilyl derivative (Fig. 1 and Table 2) and its SiSi bond of 240 pm length, a Pauling bond order of 0.83 is derived, which fits into the linear regression (Fig. 2) based on known literature values [18,25,26]. The correlation also reveals the 35 pm range for Si–Si single bond lengths.

It has been suggested that the reduced Si–Si skeletal bond orders are presumably compensated by van der Waals bonding contributions within the "peripheral H$_3$C skin" [25,26], illustrated here by a space-filling representation of the title compound structure (Fig. 1) with hydrogen radii in one case restricted to 32 pm
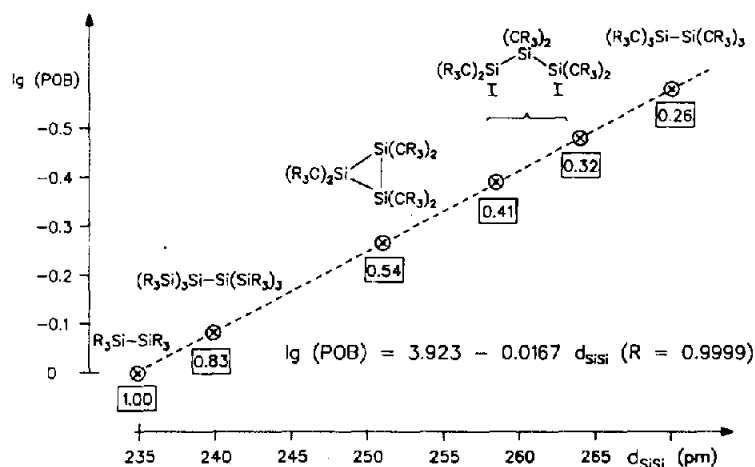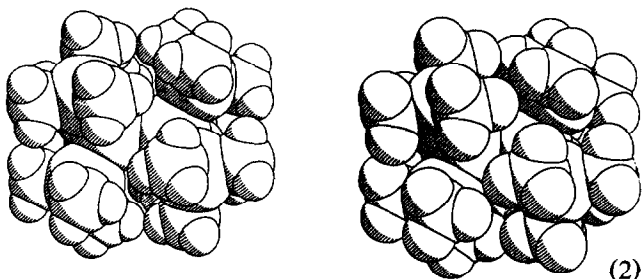

Fig. 2. Correlation of Pauling Bond Orders and SiSi bond lengths lgPOB/d_{SiSi} for sterically overcrowded di- and tri-silane derivatives (R = CH$_3$. □, bond orders).

and in the other as upscaled to more realistic ones of 52 pm:

(2)

If so, then sterically overcrowded organosilicon molecules provide another example of van der Waals attraction, which is a facet of considerable importance for molecular recognition and self-organization, especially in biochemical processes [28].

4. Photoelectron spectrum in the gas phase

The He(I) photoelectron spectrum of $[(H_3C)_3Si]_3Si$-$Si[Si(CH_3)_3]_3$ (Fig. 3), a high melting solid, had to be recorded at 350 K using a heated inlet system [29]. It shows three ionization hills of numerous overlapping bands between 7.3 and 9.1 eV, 9.3 and 11.5 eV and 16.0 eV. To provide some guidelines in their assignment via a comparison of radical cation states, $[(H_3C)_3Si]_3SiCl$ was also prepared (Experimental Section) and its photoelectron spectrum (Fig. 4) recorded.

For the rather large title molecule $C_{18}H_{54}Si_8$, according to a useful counting rule of element p and hydrogen 1s electrons [29], $\Sigma(np_E) + 1s_H)/2$, more than 50 ionizations are expected to crowd within the He(I) measurement region. To start with the low-energy-band hill, a photoelectron spectroscopic comparison with other permethylpolysilanes [29,32,33] and especially the low effective nuclear charge of silicon [33] provide clear-cut evidence for radical cation states with dominant σ_{SiSi} contribution. Their tentative assignment begins with an AM 1 calculation using the experimentally determined coordinates (Table 1), which yields for the lowest occupied molecular orbitals with large Si contributions the eigenvalues -9.25 (26e), -10.01 (25e), -9.82 (15a$_1$),m -10.75 (12a$_2$) and, after the following 12 orbitals of σ_{SiC} character, another one at -11.84 eV (12a$_1$). Therefore, in the low-energy-band hill presumably six overlapping bands are located, of which four are most likely Jahn–Teller-split $\pi(e)$-type ionizations, one of localized $\sigma_{SiSi}(a_2)$-character and one of more delocalized $\sigma(a_1)$-character. The qualitative band analysis (Fig. 3, insert: $\cdots$) thus aims to simulate the sharper π- and the usually rather flat σ-band contours. The outlying low energy flank of the ionization hill, which is not considered in the band
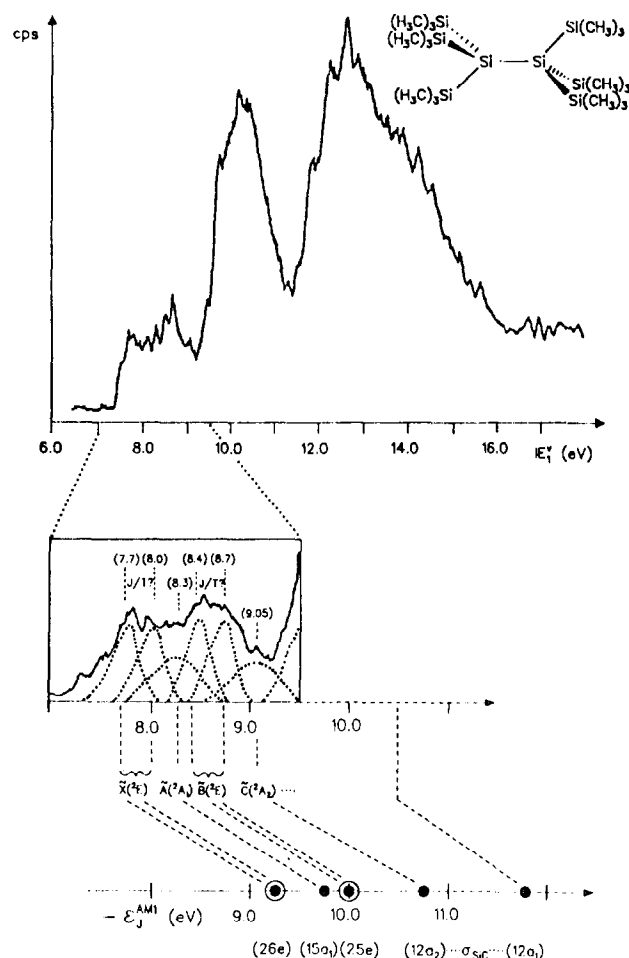

Fig. 3. He(I) photoelectron spectrum 6 eV to 18 eV of hexakis(trimethylsilyl)disilane at 350 K and (insert) expanded scan of the region 7–9.5 eV, together with a tentative assignment for the radical cation states of the $Si_3SiSiSi_3$ skeleton of D_3 symmetry based on Koopmans' correlation with AM 1 eigenvalues (cf. text).

shape evaluation, may be due to either rotational conformers of near D_{3h} symmetry or to potential thermal fragmentation products such as, possibly, tetrakis(trimethylsilyl)disilene. The somewhat larger Koopmans' deviations, $\Delta(\epsilon_j^{AM1} - IE_n^v)$, of about 1.3 to 1.5 eV can be rationalized in terms of the small difference between M and M$^{\cdot+}$ correlation energies overcompensated by a considerable electronic radical cation stabilization, as indicated by the AM 1 charge distribution for the neutral molecule [34]:

(3)
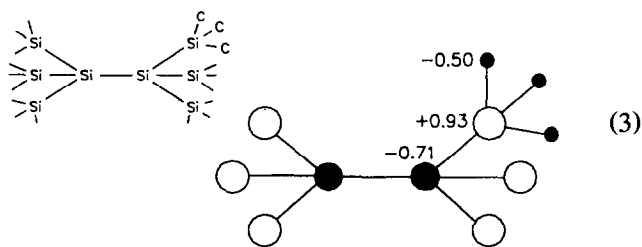
The differing charges calculated for the individual silicon centers further illustrate that the title compound does contain two different σ_{SiSi} bonds: six of them, which are $(H_3C)_3$-polarized as in linear or cyclic methyl polysilanes [29,30,32], and a special central one, which seems to be electron-rich but is surrounded by six positively charged Si centers.

The tentative assignment of the seven Si–Si ionizations in hexakis(trimethyl)disilane (Fig. 3, insert) covers all spectroscopic observations, and is in accordance with the AM 1 calculation for the 70 atom-molecule based on the experimental structure. It is further supported by an LCBO-MO model [29,32,33], in which the two different Si–Si bonds are parametrized as follows. For the six outer σ_{SiSi} bonds the well-tested Coulomb value, $\alpha_{SiSi} = 8.7$ eV, and for all geminal SiSi interactions the resonance integral, $\beta_{SiSi/SiSi} = 0.5$ eV, resulting from a linear correlation for straight-chain, branched and cyclic polysilanes are used again [29,32,33]. For the central Si–Si bond surrounded by six positively charged Si centers (3), a higher Coulomb parameter of $\alpha_{SiSi} \approx 9.05$ eV is assumed, and for the
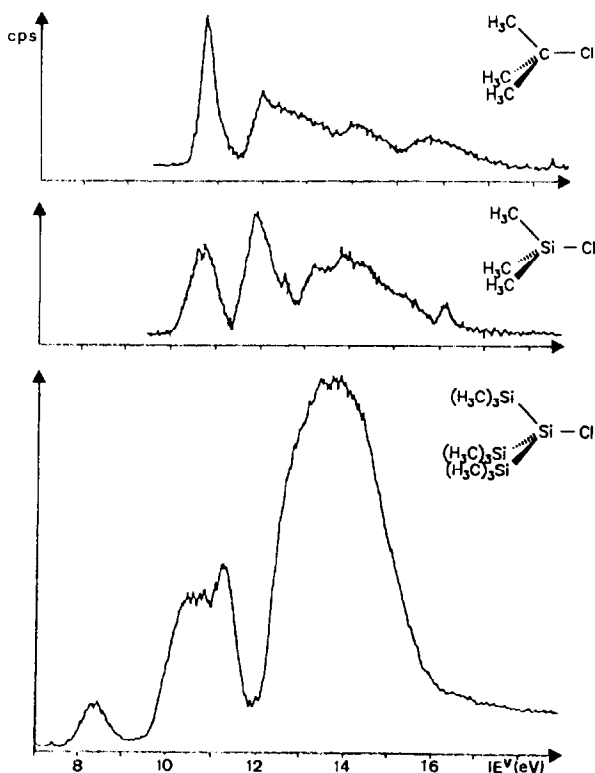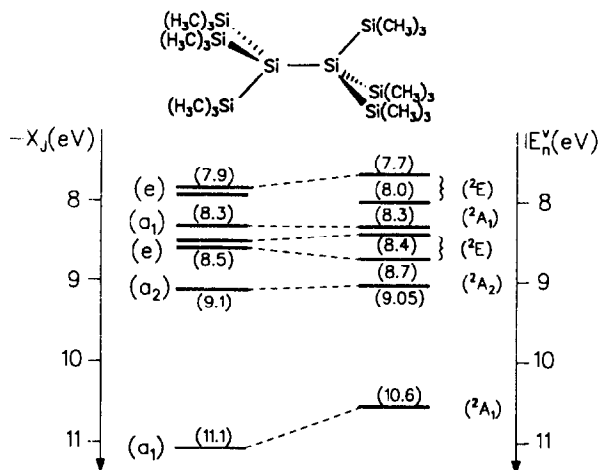

Fig. 5. Correlation of topological eigenvalues x_j from a LCBO-MO model for the Si–Si skeleton of hexakis(trimethylsilyl)disilane (cf. text) and its PE-spectroscopically-determined vertical ionization energies IE_n (Fig. 3, insert).


Fig. 4. He(I) photoelectron spectra of tris(trimethylsilyl)chlorosilane, trimethylchlorosilane [29], and t-butyl chloride [30,31].

additional π interaction between adjacent vicinal Si–Si bonds a smaller resonance term $\beta_{SiSi-SiSi} \approx 0.3$ eV. For the seven expected Si–Si skeletal orbitals of the reducible representation $\Gamma = 2a_1 + 1a_2 + 2e$, this reasonable parametrization yields a topological eigenvalue scheme (Fig. 5), which correlates satisfactorily with the PES ionization pattern, as deduced from the combination of band shape analysis and Koopmans' assignment based on AM 1 eigenvalues (Fig. 3, insert).

Comparison of the radical cation states of a great variety of polysilanes [29,32,33], including the title compound of D_3-symmetry, further substantiates the delocalization of positive charges along Si–Si links, first predicted in 1971 [32], and the band structures for solid $(SiR_2)_n$ polymers established since then [33,35].

The second ionization hill contains most of the overlapping bands of the 18 predominantly σ_{SiC}-type ionizations [29]. The rest of them together with the 36 expected ionizations into $M^{·+}$ states with dominant σ_{CH_3} contributions [29] form the very large ionization mountain between 11.5 eV and 16 eV (Fig. 3). Due to the density of $M^{·+}$ states around both 10.3 eV and 13 eV, any attempt to assign individual ionizations by Koopmans' correlation, $IE_n^v = -\epsilon_j^{AM1}$, based on AM 1 eigenvalues would be pointless. Their overall classification, however, can be further substantiated by a comparison with equivalent $M^{·+}$ states of chemically related molecules [36] such as $[(H_3C)_3Si]_3SiCl$, $(H_3C)_3SiCl$ and $(H_3C)_3CCl$ (Fig. 4).

For t-butylchloride, an ab initio calculation with a relatively large basis set suggests the following Koop-

mans' assignment of its photoelectron spectrum [31] (Fig. 3):

$$ (4) $$
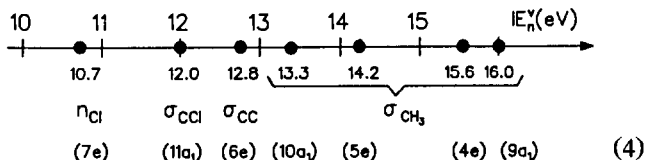
The interaction between the highest two occupied e-type molecular orbitals (4: 7e and 6e) is defined as n_{Cl}/σ_{ER_3} hyperconjugation [29,36] in terms of second order perturbation [37], $\delta\epsilon_j \approx \beta^2_{Cl/ER_3}/(\alpha_{ER_3} - \alpha_{Cl})$, and conveniantly estimated by inserting suitable photoelectron spectroscopic ionization energies into a second order interaction determinant [29,36]:

$$ \begin{vmatrix} \alpha_1 - \epsilon_j & \beta_{21} \\ \beta_{12} & \alpha_2 - \epsilon_j \end{vmatrix} = 0 \rightarrow $$

$$ \beta^\pi_{Cl/ER_3} = \sqrt{(\alpha^\pi_{Cl} - IE_1^v)(\alpha^\pi_{ER_3} - IE_1^v)} \quad (5) $$

With $\alpha_{Cl} = -12.80$ eV (from HCl [31]), $\alpha_{CH_3} = -14.20$ eV (from H_3C-CH_3 [31]) and $\alpha_{SiH_3} = -12.80$ eV (from H_3SiSiH_3 [32]), the hyperconjugation parameters $\beta_{Cl/CH_3} = -2.1$ eV and $\beta_{Cl/SiH_3} = -1.1$ eV result [29,32,36]. The lower Coulomb parameter α_{SiH_3} reflects the smaller effective nuclear charge of silicon [29,36], and the considerably smaller hyperconjugative interaction parameter β_{Cl/SiH_3}, the larger SiCl bond distance, i.e. the reduced overlap of the $\pi(e)$-type molecular orbitals [29].

In the photoelectron spectrum of the iso(valence) electronic trimethylchlorosilane [29] (Fig. 4), the sequence of the first three M·+ states is changed to $\sigma_{SiC_3}(e) < n_{Cl}(e) < \sigma_{SiCl}$, an assignment, supported, e.g. by the visible 0.15 eV Jahn-Teller split of the first photoelectron band (Fig. 4) or the lower $\sigma_{SiC_3}(e)$ ionization energy of $(H_3C)_3SiH$ ($IE_1^v = 10.7$ eV [29]) relative to $\sigma_{CC_3}(e)$ of $(H_3C)_3CH$ ($IE_2^v = 11.9$ eV [31]). As concerns the hyperconjugative interaction parameters, a crude estimate based on comparison of the respective R_3E-H and R_3E-Cl ionization energies in their inverted sequence would yield the considerably smaller values $\beta_{Cl/CR_3} \approx -1.2$ eV and $\beta_{Cl/SiR_3} \approx -0.3$ eV. It must be pointed out, however, that in larger molecules with several M·+ states of the same irreducible representation, hyperconjugation cannot be as straightforwardly defined.

On the basis of preceding discussion, the total of 32 expected valence ionizations of $[(H_3C)_3Si]_3SiCl$ within the He(I) measurement region (Fig. 4) are assigned as follows. The low-energy band with an 8.5 eV maximum belongs to the radical cation ground state with predominant $\sigma_{SiSi_3}(e)$ contribution, and is lowered by as much

as 2.3 eV relative to the corresponding $\sigma_{SiC}(e)$ ionizations of $(H_3C)_3SiCl$, thereby again demonstrating the tremendous effect of the smaller Si effective nuclear charge. The ionization hill between 9.7 eV and 11.7 eV should comprise the $\sigma_{SiSi_3}(a_1)$ as well as 6 σ_{SiC} ionizations, and presumably shows on its high energy flank the usually somewhat "sharper" $n_{Cl}(e)$ ionization needle with its maximum at 11.2 eV, i.e. lowered by ca. 0.7 eV relative to that of $(H_3C)_3SiCl$. Although hyperconjugation cannot be defined in a molecule such as $[(H_3C)_3Si]_3SiCl$ because of its numerous $\pi(e)$-type radical cation states, comparison with the LCBO-MO model for the title compound (Fig. 5) and its parametrization suggests a rather small $n_{Cl}/\sigma_{SiSi_3}(e)$ interaction, because the difference in the Coulomb values, $\alpha_{Cl} - \alpha_{Si(Si)_3}$, presumably exceeds 2.5 eV. The huge ionization mountain between 12.2 eV and 16.0 eV presumably contains the overlapping bands of one $\sigma_{SiCl}(a_1)$, three σ_{SiC} and 18 σ_{CH_3} dominated M·+ states, together with additional ones with increasing $3s_{Si}$ contribution.

Returning to the PE spectroscopic discussion of the title molecule, the radical cation state comparison with the halogen derivatives (Fig. 5) supports the assignment of the three ionization hills to radical cation states of predominant σ_{SiSi} contributions in the first one (Fig. 5), those of $\sigma_{SiC}(+\sigma_{SiSi})$ character in the second, and those arising from delocalization of the positive charge largely into $\sigma_{CSi} + \sigma_{CH}$ bonds to the biggest one. The first ionization energy of $[(H_3C)_3Si]_3$ $Si-Si[Si(CH_3)_3]_3$ is lowered by 0.54 eV relative to that of $[(H_3C)_3Si]_4Si$ ([29]: 8.24 eV). Relative to the values for other simple open-chain disilane derivatives [29] such as

$$ (6) $$
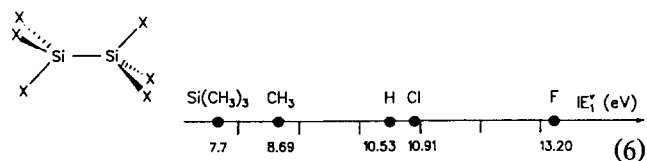
it is by far the lowest measured so far. Diagram (6) also reveals impressively how sensitive the "electron-rich" Si-Si bond is to electron withdrawal by substituents X of higher effective nuclear charge: the differences in first vertical ionization energies amount to as much as 5.7 eV.

5. Additional cyclovoltammetric measurements

A great variety of organosilicon compounds with low first vertical ionization energies [29,33,38] can be oxidized in aprotic solution to their radical cations, especially by use of the powerful single electron transfer reagent $AlCl_3/H_2CCl_2$ [39]. Many of them are persis-
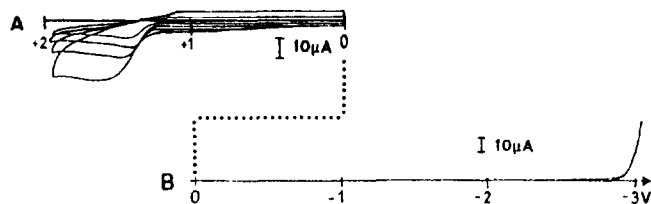
Fig. 6. Cyclovoltammograms of $(R_3Si)_3SiSi(SiR_3)_3$ at 295 K. (A) Oxidation between 0 and $+2$ V $(H_2CCl_2/0.1$ M $R_4N^+ClO_4^-$; GCE vs. Ag/AgCl; $v = 50$ to 500 mV s^{-1}). (B) Reduction between 0 and -3V (dimethylformamide/0.1 M $R_4N^+ClO_4^-$; GCE vs. Ag/AgCl; $v = 100$ mV s^{-1}).

tent, at least at low temperatures, and thus can be characterized by their ESR and ENDOR spectra [38], including ^{29}Si isotope ENDOR spectra [40]. For hexakis(trimethylsilyl)disilane, with its rather low first vertical ionization energy of only 7.70 eV (5), a 'thermodynamically' feasible oxidation to its radical cation is thus expected.

Cyclovoltammetric measurements in $H_2CCl_2/R_4N^+ClO_4^-$ under aprotic conditions (experimental section), however, demonstrate that the oxidation at about $+1.4$ V occurs irreversibly, and that the peak potential at about $+1.2$ V is "kinetically" dependent on the recording velocity (Fig. 6A: 1.40 V at 50 mV s^{-1} to 1.54 V at 500 mV s^{-1}).

Furthermore (Fig. 6B), no reduction occurs below -3 V. Despite these disappointing cyclovoltammetric results, preparative oxidation in an ESR cavity was attempted at 200 K using as single electron acceptor reagents $AlCl_3/H_2CCl_2$, $NO^+BF_4^-/H_3CCN$, $F_3CCO_2^-Ag^+/H_2CCl_2$ and $(BrC_6H_4)_3N^+SbCl_6^-$. Although the aprotic solution turned yellowish, no ESR signals could be detected. An additional reduction experiment in a THF solution containing [2.2.2]-cryptand by use of a highly reactive potassium mirror also produced no observable paramagnetic species.

Acknowledgments

References

1 H. Bock, J. Meuret and K. Ruppert *Angew. Chem.*, (1993) in press. This article is also Part CXXXVI of the series Photoelectron Spectra and Molecular Properties. For Part CXXXV see

O. M. Nefedov, V. A. Korolev, L. Zanathy, B. Solouki and H. Bock, *Mendelejev Commun.*, (1992) 67.

2 (a) J. Meuret, *Ph.D. Thesis*, Frankfurt University, 1992.

3 (a) H. Gilman and C. L. Smith, *J. Am. Chem. Soc.*, *86* (1964) 1454; (b) H. Gilman and C. L. Smith, *J. Organomet. Chem.*, *8* (1967) 245; (c) H. Gilman, J. M. Holmes and C. L. Smith, *Chem. Ind. (London)*, *15* (1965) 848; (d) H. Gilman and R. L. Harrell, *J. Organomet. Chem.*, *5* (1966) 199; (e) H. Gilman and R. L. Harrell, *J. Organomet. Chem.*, *9* (1967) 67; (f) H. Gilman and C. L. Smith, *J. Organomet. Chem.*, *14* (1968) 91.

4 A. G. Brook, S. Nyberg, F. Abdesaken, B. Gutekunst, R. K. M. R. Kallury, Y. C. Poon, Y.-M. Chang and W. Wong-Ng, *J. Am. Chem. Soc.*, *104* (1982) 5668 and references cited therein.

5 M. Haase, U. Klingebiel, R. Boese and M. Polk, *Chem. Ber.*, *119* (1986) 1117.

6 F. H. Elsner, H.-G. Woo and T. D. Tilley, *J. Am. Chem. Soc.*, *110* (1988) 314.

7 See C. Chatgilialoglu, D. Griller and M. Lesage, *J. Org. Chem.*, *54* (1989) 2492. K. J. Kulicke and B. Giese, *Synlett. 91* (1990); C. Chatgilialoglu, *Acc. Chem. Res.*, *25* (1991) 188.

8 L. S. Bartell, F. B. Clippard, Jr., and T. L. Boates, *Inorg. Chem.*, *9* (1970) 2436.

9 M. C. Couldwell, J. Simpson and W. T. Robinson, *J. Organomet. Chem.*, *107* (1976) 323; B. K. Nicholson, J. Simpson and W. T. Robinson, *J. Organomet. Chem.*, *47* (1973) 403 and references cited therein.

10 J. Arnold, T. D. Tilley, A. L. Rheingold and S. G. Geib, *Inorg. Chem.*, *26* (1987) 2106.

11 For some interesting organometallic derivatives (*cf.* the review by W. S. Sheldrick, in S. Patai and Z. Rappoport (eds.), *Chemistry of Organic Silicon Compounds* Wiley, Chichester, 1989, pp. 227–303) angles MeSiSi are not reported for *e.g.* $[(R_3Si)Si]_2Sn \cdot LiCl(THF)_3$ (A. M. Arif, A. H. Cowley and T. Elkins, *J. Organomet. Chem.*, *325* (1987) C11) or $[R_3Si)_3Si]_2In(\mu-Cl)_2Li(THF)_2$ (A. M. Arif, A. H. Cowley, T. M. Elkins and R. A. Jones, *J. Chem. Soc.*, *Chem. Commun.* (1986) 1776).

12 (a) R. H. Heyn and T. D. Tilley, *Inorg. Chem.*, *28* (1989) 1768; (b) J. Meyer, J. Willnecker and U. Schubert, *Chem. Ber.*, *122* (1989) 223.

13 (a) M. H. Chisholm, H.-T. Chin, K. Folting and J. C. Huffmann, *Inorg. Chem.*, *23* (1984) 4097; (b) S. P. Mallela and R. A. Geanangel, *Inorg. Chem.*, *29* (1990) 3525 and references cited therein.

14 H. Bock, J. Meuret, R. Baur and K. Ruppert, *J. Organomet. Chem.*, (JOM 23030) in press.

15 (a) N. Wiberg, H. Schuster, A. Simon and K. Peters, *Angew. Chem.*, *98* (1986) 100; *Angew. Chem. Int. Ed. Engl.*, *25* (1986) 79; (b) N. Wiberg, E. Kühnel, K. Schurz, H. Borrmann and A. Simon, *Z. Naturforsch.*, *43B* (1988) 1075.

16 H. Bock, J. Meuret and K. Ruppert, *Organometallics*, unpublished results.

17 (a) M. J. S. Dewar, E. G. Zoebisch, E. F. Healy and J. P. Stewart, *J. Am. Chem. Soc. 107* (1985) 3902; (b) M. J. S. Dewar and J. Caoxian, *Organometallics*, *6* (1987) 1486.

18 H. Bock, K. Ruppert, C. Näther, Z. Havlas, H.-F. Herrmann, C. Arad, I. Göbel, A. John, J. Meuret, S. Nick, A. Rauschenbach, W. Seitz, T. Vaupel and B. Solouki, *Angew. Chem.*, *104* (1992) 564; *Angew. Chem., Int. Ed. Engl.*, *31* (1992) 550.

19 B. Beagley, A. R. Conrad, J. M. Freeman, J. J. Monaghan, B. G. Morton and G. C. Holywell, *J. Mol. Struct.*, *11* (1972) 371.

20 H. Oberhammer, *J. Mol. Struct.*, *31* (1976) 237 and references cited therein.

21 D. W. H. Rankin and A. Robertson, *J. Mol. Struct.*, *27* (1975) 438.

22 J. Haase, *Z. Naturforsch., 28a* (1973) 542 and references cited therein.

23 B. Beagley, J. J. Monaghan and T. G. Hewitt, *J. Mol. Struct. 8* (1971) 401.

24 Y. Morino and E. Hirota, *J. Chem. Phys., 28* (1958) 185.

25 A. Schäfer, M. Weidenbruch, K. Peters and H. G. v. Schnering, *Angew. Chem., 96* (1984) 311; *Angew. Chem., Int. Ed. Engl., 23* (1984) 302.

26 M. Weidenbruch, B. Flintjer, K. Peters and H. G. v. Schnering, *Angew. Chem., 98* (1986) 1090; *Angew. Chem., Int. Ed. Engl., 25* (1986) 1129.

27 L. Pauling, *The Nature of the Chemical Bond*, Cornell University Press, 1960.

28 W. Kaim and B. Schwederski, *Bioorganische Chemie*, Teubner, Stuttgart, 1991.

29 H. Bock and B. Solouki, Photoelectron spectra of silicon compounds, in S. Patai and Z. Rappoport (eds.), *The Chemistry of Organic Silicon Compounds*, Wiley, Chichester, 1989, pp. 555–653 (and references cited therein).

30 K. Wittel and H. Bock, Photoelectron spectra of organic halogen compounds, in S. Patai and Z. Rappoport (eds.), *The Chemistry of Functional Groups, Supplement D*, Wiley, Chichester 1983, pp. 1499–1603 (and references cited therein).

31 K. Kimura, S. Katsumata, Y. Achiba, T. Yamazaki and S. Iwata, *Handbook of the He(I) Photoelectron Spectra of Fundamental Organic Molecules*, Halstead Press, New York, 1981, and references cited therein.

32 H. Bock and W. Enßlin, *Angew. Chem., 83* (1971) 435; *Angew.*

Chem. Int. Ed. Engl., 10 (1971) 404; H. Bock, W. Enßlin, F. Feher and R. Freund, *J. Am. Chem. Soc., 98* (1976) 668; not cited in R. West, Polysilanes, in S. Patai and Z. Rappoport (eds.), *The Chemistry of Organic Silicon Compounds*, Wiley, Chichester, 1989, pp. 1208–1240.

33 H. Bock, Fundamentals of silicon chemistry: molecular states of silicon-containing compounds, *Angew. Chem., 101* (1989) 1659; *Angew. Chem. Int. Ed. Engl., 18* (1989) 1627.

34 H. Bock, J. Meuret and U. Stein, *J. Organomet. Chem., 398* (1990) 65.

35 K. Takeda, H. Teramae and N. Matsumoto, *J. Am. Chem. Soc., 108* (1986) 8186. H. Teramae and K. Takeda, *J. Am. Chem. Soc., 111* (1989) 1281.

36 H. Bock, Molecular states and molecular orbitals, *Angew. Chem., 89* (1977) 631–655; *Angew. Chem. Int., Ed. Engl., 16* (1977) 613–637 and references cited therein; W. Enßlin, H. Bock and G. Becker, *J. Am. Chem. Soc., 96* (1974) 2757.

37 E. Heilbronner and H. Bock, *The HMO Model and its Application*, Vol. 1, German edn., Verlag Chemie, Weinheim 1978 (English translation: Wiley, London, 1976. Japanese translation: Hirokawa, Tokyo, 1973. Chinese translation: Kirin University Press, 1982).

38 H. Bock and W. Kaim, Organosilicon radical cations, *Acc. Chem. Res., 15* (1982) 9 and references cited therein.

39 H. Bock and U. Lechner-Knoblauch, *J. Organomet. Chem., 294* (1985) 295.

40 H. Bock, B. Hierholzer, H. Kurreck and W. Lubitz, *Angew. Chem., 95* (1983) 817; *Angew. Chem. Int. Ed. Engl., 22* (1983) 787.